Int J Adv Manuf Technol (2013) 67:601–611
DOI 10.1007/s00170-012-4508-2

ORIGINAL ARTICLE

Using specially designed high-stiffness burnishing tool to achieve high-quality surface finish

Branko Tadic · Petar M. Todorovic · Ognjan Luzanin · Dragomir Miljanic · Branislav M. Jeremic · Bojan Bogdanovic · Djordje Vukelic

Received: 16 May 2012 / Accepted: 6 September 2012 / Published online: 18 September 2012

Abstract This paper is focused on the process of ball burnishing. The influence of tool stiffness on surface roughness parameters was considered theoretically, while experimental investigation was conducted to establish the influence of initial surface roughness (previous machining) on the effects of ball burnishing as the finishing process. Experimental investigations were conducted over a wide interval of most influential process parameters (burnishing forces, burnishing feed, and number of burnishing passes). The material used in the experiments was aluminum alloy EN AW-6082 (AlMgSi1) T651. Burnishing was performed using a specially designed tool of high stiffness. Statistical analysis of experimental data revealed strong correlation between roughness, R_a, and burnishing force, burnishing feed, and number of passes for the three surfaces, each with different roughness parameters. Particular combinations of process parameters yielded very low surface roughness, R_a, equivalent to polishing. It is worth noting that high surface quality can be achieved with relatively small burnishing forces, which differs from the investigations published so far. Contrary to conventional approaches, which are based on elastic tool systems, the authors propose the burnishing process to be conducted with high-stiffness tools. Further investigation shall be focused on optimization of burnishing process parameters in order to achieve surface finish equivalent to high polish.

Keywords Ball burnishing · Tool stiffness · Surface roughness

B. Tadic · P. M. Todorovic · B. M. Jeremic · B. Bogdanovic
Department for Production Engineering, Faculty of Engineering, University of Kragujevac,
34000 Kragujevac, Serbia

O. Luzanin · D. Vukelic (✉)
Department for Production Engineering, Faculty of Technical Sciences, University of Novi Sad,
21000 Novi Sad, Serbia
e-mail: vukelic@uns.ac.rs
URL: http://www.ftn.uns.ac.rs/

D. Miljanic
Metalik DOO,
81400 Niksic, Montenegro

1 Introduction

Surface roughness has a significant impact on performance of mechanical components [1]. Regardless of the machining or forming technology applied (turning, milling, grinding, rolling, casting, forging, etc.) processed surfaces of mechanical components always feature roughness, which directly impacts their interaction with the assembly [2]. Quality finishing has positive impact on the functioning of mechanical assemblies, power transmission, resistance to wear, corrosion, operating life of mechanical assemblies, and fatigue strength [3]. Conversely, inadequate finishing primarily inflates energy consumption, increases wear, and the risk of poor tolerances [4]. Among the most frequently used processes for the increase in surface roughness are fine turning and milling, grinding, polishing, honing, lapping, superfinish, etc. Another parameter that determines surface quality is surface microhardness, which largely influences wear resistance and fatigue strength. Alternative methods aimed at achieving higher wear resistance and fatigue strength are based on pure deformation strengthening [5]. Mechanical processes that are often used to increase fatigue strength are shot peening, hammering, water-jet peening, brushing, ballizing of bores, and autofrettage.

One of the finishing methods that does not rely on chip removal is ball burnishing. This method increases surface quality, surface hardness, and dimensional accuracy [6, 7]. In addition, it reduces surface defects and modifies microstructure of machined surfaces [5, 8–13]. Ball burnishing process involves the rolling of burnishing tool across workpiece surface. Depending on tool design, i.e., whether a ball or a roller is used as the rolling element, one can distinguish between the two processes: ball burnishing and roller burnishing.

Literature review reveals that, in comparison to machining, burnishing offers specific advantages such as improved surface roughness and hardness [1, 6, 14–17], which result in increased corrosion resistance [18, 19], wear resistance [19, 20], fatigue strength [17, 21], and tensile strength [22]. In addition, burnishing also contributes to transformation of surface tensile stresses—which are the result of previous machining (turning, milling, etc.)—into compression stresses, which improves several mechanical properties [22–25]. The depth of penetration of compression stresses, as well as the thickness of the hardened surface layer, depends on workpiece material and applied loads.

Burnishing can be used on various workpiece materials such as various steels [1, 4, 5, 8, 9, 15, 25], bronze [6], alloys for special applications [26], and aluminum [15, 22, 23], on inner and outer surfaces of cylindrical workpieces, as well as on the small- and large-area flat surfaces.

The burnishing process has been studied by numerous researchers who investigated the effects of workpiece material, tool material (ball or roller), tool geometry, type of contact, and various process parameters. The parameters of burnishing process include burnishing speed, burnishing feed, burnishing force (pressure), and the number of burnishing passes. A majority of reports search for a combination of process parameters for various materials, which allow optimal results [1, 4, 6, 10, 14, 22–24, 27]. El-Taweel and El-Axir [6] examined bronze burnishing and established that burnishing force, feed, speed, and the number of passes exert greatest influence on workpiece surface roughness and hardness. They established that higher burnishing force and number of passes are associated with the increase in hardness, while hardness can also be increased at lower burnishing speeds and feed rates. El-Taweel and El-Axir used Taguchi method to limit the number of experiments and reliably determine optimal burnishing parameters. Gharbi et al. [1] used AISI 1010 steel plates for burnishing and established that burnishing force was the most influential parameter, followed by speed, feed rate, and number of passes. Experimenting with AISI 1010 plates, they also established that the burnishing force should not exceed 400 N in order to prevent peeling of surface layers. Their experiments also revealed that increased burnishing force results in thicker layers of strengthened material. Beside the force, which is the most important factor of the burnishing process with the decisive role in the peeling (damaging) of workpiece surface layers, the number of passes also influences surface roughness and hardness and influences the occurrence of surface defects [12, 13, 28]. In addition, Gharbi et al. [1, 22] developed mathematical models able to predict surface roughness and hardness as the result of burnishing. Working with soft steel and aluminum, Nemat and Lyons [15] established that surface roughness can be improved up to 70 % by adjusting the burnishing parameters, while the reduction of burnishing speed and feed rate led to increased hardness of both materials. Generally, burnishing improves surface roughness between 40 and 90 % [27, 29–34]. Lin et al. [4] proposed the burnishing factor, L_b, as the parameter that defines the optimal combination of burnishing parameters. Burnishing factor, L_b, is a function that depends on workpiece material hardness, maximum contact pressure, relative sliding speed between workpiece surface and tool, dynamic viscosity of lubricant, characteristics of lubricant additives, and a correction factor of the boundary film. This correction factor allowed them to establish the relationship between surface roughness, burnishing factor, initial value of workpiece surface roughness, tool surface roughness, and burnishing feed.

Analysis of published work reveals different tool designs, which utilize work elements in the shape of ball or roller. The ball and roller can be made from ceramics, wolfram carbide, chrome carbide, high chromium structural steels, etc. The tools are designed so that the work element is allowed freedom of movement. This is mostly achieved by ancillary balls, which support the work element [1, 6, 22], preventing the formation of adhesive joints. Tool designs mostly utilize elastic springs to apply or measure burnishing force [1, 6, 15, 22]. There are also design solutions that provide the required force by means of pressurized fluid [5, 8, 9]. Finally, there are some special solutions which use flexible tool holders [4].

In contrast to previous investigations, the authors of this paper discuss the effects of the burnishing process taking into consideration the initial surface roughness, i.e., workpiece condition due to previous machining. Another thing that distinguishes this work from the others is that the burnishing was performed with a specially designed tool of high stiffness. More precisely, based on theoretical considerations, the authors assumed that, compared to its previous counterparts with springs, a high-stiffness tool should increase surface quality. Especially large percentage increase in surface quality was observed in the case of workpieces, which entered the burnishing process with rougher surfaces. Extensive experimental work was performed in order to support the claims.

2 Theoretical analysis

Beside parameters that define cutting regime and other conditions (state of machine tool, machining fixtures, lubrication, etc.), the tool has a crucial role in any machining process. The authors of this paper maintain that investigations in the field of burnishing should be mostly focused on the analysis of dynamic tool behavior. This is especially important in cases of high-speed machining, e.g., burnishing on a lathe. Available literature does not provide information on any thorough theoretical analysis of tool behavior under real machining conditions. For example, one is unable to find the stiffness data on springs, which provide burnishing force [1, 6, 15, 22], or the data on pressure and variation of fluid, which provides contact force between the burnishing ball and workpiece [5, 8, 9]. However, it should be noted that dynamic tool behavior during burnishing process is very difficult to define theoretically. This is especially true bearing in mind that the process is performed over uneven surfaces while the dispersion of excitation forces, which act on the tool is unknown. In addition, the magnitudes of tool displacement into roughness valleys are on a microscopic order. Through the following theoretical investigation, the authors attempt to shed a global light on the values that are tool related and impact the output effects of the burnishing process. A treatment of flat surface area is considered at relatively low tool speeds. Figure 1 illustrates the burnishing tool in contact with workpiece material.

The force required for burnishing is applied by a spring of stiffness k. In order to apply the force F, prior to beginning of the burnishing process, the spring is compressed by a static displacement, f_{st}, from the referential position A_1A_1, into position A_2A_2. The contact between the ball and workpiece material during tool movement along x-axis begins at roughness peaks, e.g., at points K_1 and K_2, in the direction defined by the angle of ball engagement, φ_z. Due to stochastic nature of roughness, the angle of ball engagement, φ_z, varies also, as well as the resulting resistance, F_R, which at times t_1 and t_2 equals $F_R(t_1)$ and $F_R(t_2)$. The varying resistance force shall cause oscillatory movement at one end of the spring (point B) relative to the referential position, A_2A_2, by some value, f_d. These oscillations impact the quality of surface (arithmetical mean roughness, surface waviness, and other roughness parameters). Considering the previous discussion, there holds:

$$F \pm \Delta F = k \cdot (f_{st} \pm f_d) \qquad (1)$$

from which follows:

$$f_d = \pm(\Delta F / k) \qquad (2)$$

where ΔF is the interval of force variations, and f_d is the tool (ball) displacement in z direction due to force, with the assumption of $f_d \approx A_d/2$ (Fig. 1).

Experimental investigation was conducted with a burnishing tool of high stiffness. Through preliminary experiments, it was established that application of high-stiffness burnishing tool can result in roughness below 0.2 μm and waviness of approximately 0.6 μm. From Eq. (2), it follows that, given the spring stiffness of 10^4N/m, the excitation force of just ΔF=0.01 N causes the compression of spring by 1 μm,

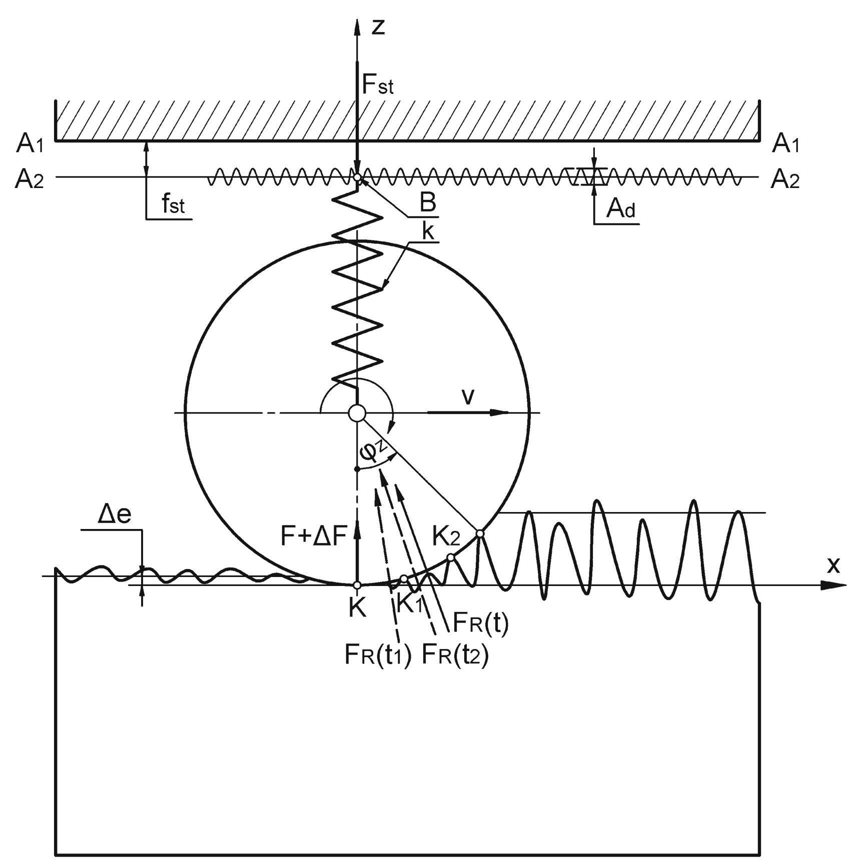

Fig. 1 Illustration of the burnishing tool in contact with workpiece material

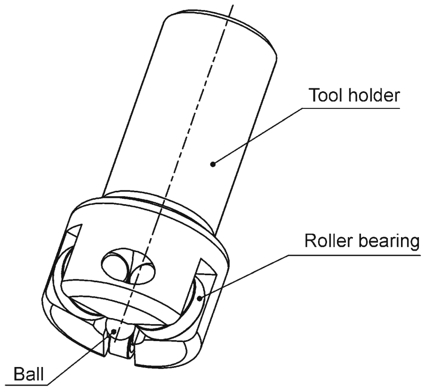

Fig. 2 3D model of the burnishing tool

which is significant for the finish roughness in burnishing. On the other hand, excitation force of ΔF=0.01 N is very likely to occur due to the stochastic nature of the roughness of previously machined surface, as well as the errors in machine tool slideways, errors in burnishing ball shape, and other tool and fixture components. Based on the previous discussion, from the aspect of surface quality and dimensional accuracy, it is best to provide the burnishing force with high-stiffness springs.

From this brief theoretical consideration, inertial and damping forces were omitted for following reasons:

- Considered in this paper is a flat surface previously machined on a numerical milling machine. It was established in preliminary experiments that surface waviness (wave step s_v) is on the order of magnitude 10^{-3}m, while the wave height is $h_v \approx 0.6$ μm. The machining was performed at 2,000 mm/min work table feed. Considering this, it was supposed that the burnishing ball oscillates over the surface waves. Based on the work table feed and the wave step, the frequency f_b and angular velocity ω of ball oscillations are approximately f_b=33.3 s^{-1}, i.e., ω=209 rad/s.
- The mass of burnishing ball used in this experiment is $m = 1.4 \times 10^{-3}$N. Knowing the mass, the amplitude of oscillations (wave height) and angular rate, one is able to calculate the inertial force:

$$F_{in} = m(h_v/2)\omega^2 = 1.8 \times 10^{-5}\,N \qquad (3)$$

It is supposed that the burnishing ball travels along surface waves following the sine curve, which means that

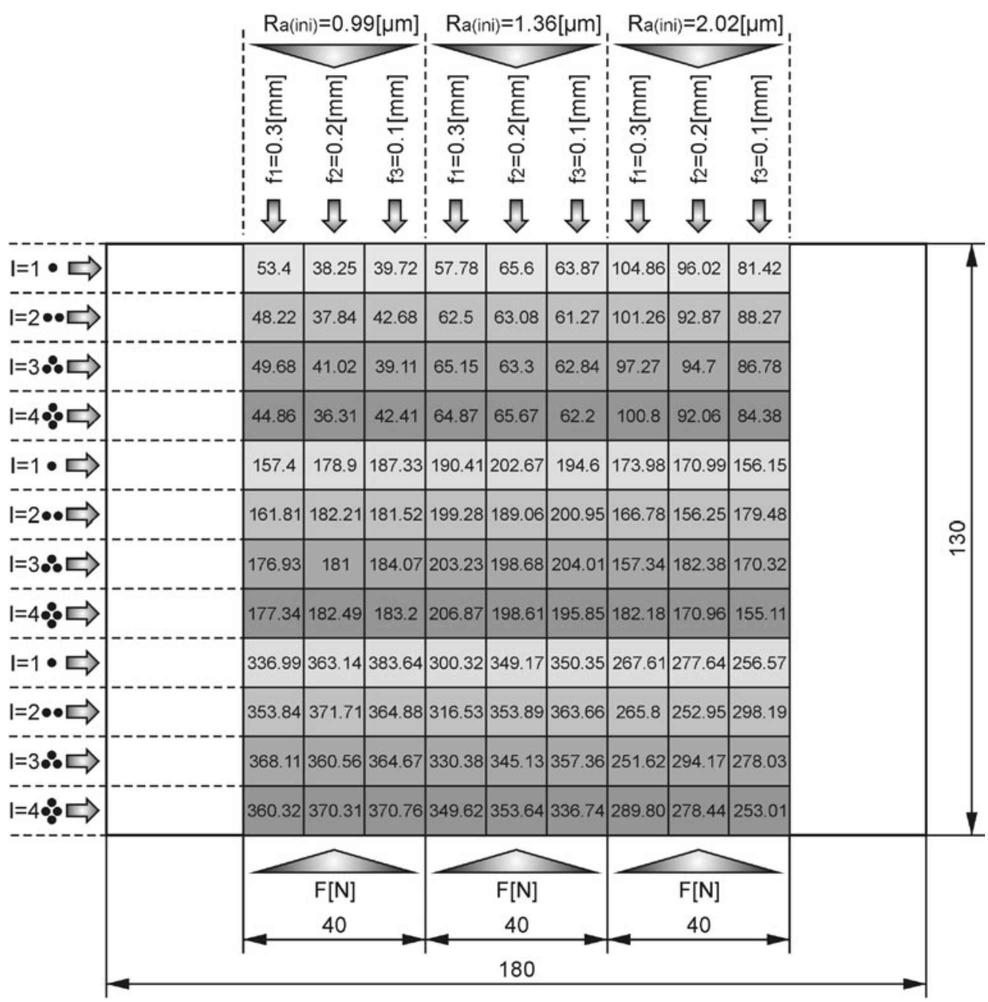

Fig. 3 Field layout of the plate used in the experiment

sine function can be used to simulate surface waviness.

- The damping force equals the product of damping coefficient and ball oscillating speed, that is:

$$F_p = b \times f_b = b(h_v/2)\omega = 6.18 \times 10^{-5} b \quad (4)$$

where b is the damping coefficient.

Considering the value of damping coefficient [35, 36], one concludes that the damping force is an order of magnitude below the spring elastic force, which is active in the course of excitation of burnishing ball.

Based on the theoretical analysis, the authors decided to conduct experiments with a high-stiffness tool. The tool (Fig. 2) is designed to provide constant depth of penetration into workpiece material, rather than the constant burnishing force. The force required for burnishing is calculated based on the depth of ball penetration into workpiece during the burnishing process. Forces were measured by Kistler dynamometer on a numerically controlled machine tool. Tool stiffness (Fig. 2) was determined through the magnitude of deformations, which are the result of contact between burnishing ball and the three radial bearings oriented at an angle of 120° relative to the direction of ball penetration into workpiece. It is clear that such tool design, with the ball supported at three points, provides rolling of the ball in xy plane. The design of burnishing tool also provides a common carrier for the radial bearings whose deformations can be neglected. In this way, total compliance of the tool system is reduced to the deformations, which occur in the zones of contact between the burnishing ball and outer rings of bearings.

3 Experimental investigation

Experimental investigation of burnishing process was conducted on a flat plate with the following characteristics: aluminum EN AW-6082 (AlMgSi1) T651, 89 HB hardness. The chemical composition was 0.9 % Si, 0.5 % Fe, 0.1 % Si, 0.6 % Mn, 0.9 %Mg, 0.25 % Cr, 0.2 % Zn, 0.1 % Ti, other elements 0.15 %, and the remaining content Al.

Dimensions of plate were 180×130×30 mm. The plate was geometrically partitioned into three sections, which were machined by milling to three different surface roughnesses. Each of the sections, 130×40 mm, was subdivided into 36 fields, to produce a total of 108 fields (Fig. 3).

Surface roughness profiles of the three sections are shown in Fig. 4. Surface roughness was measured by Talysurf 6 profilometer.

The burnishing process was performed on a numerically controlled milling machine tool using the, already described, specially designed tool. CAD model and photo image of the tool are shown in Figs. 2 and 6, respectively. The tool design features three roller bearings and allows the burnishing ball to be supported at three points and freely roll in the plane. In this

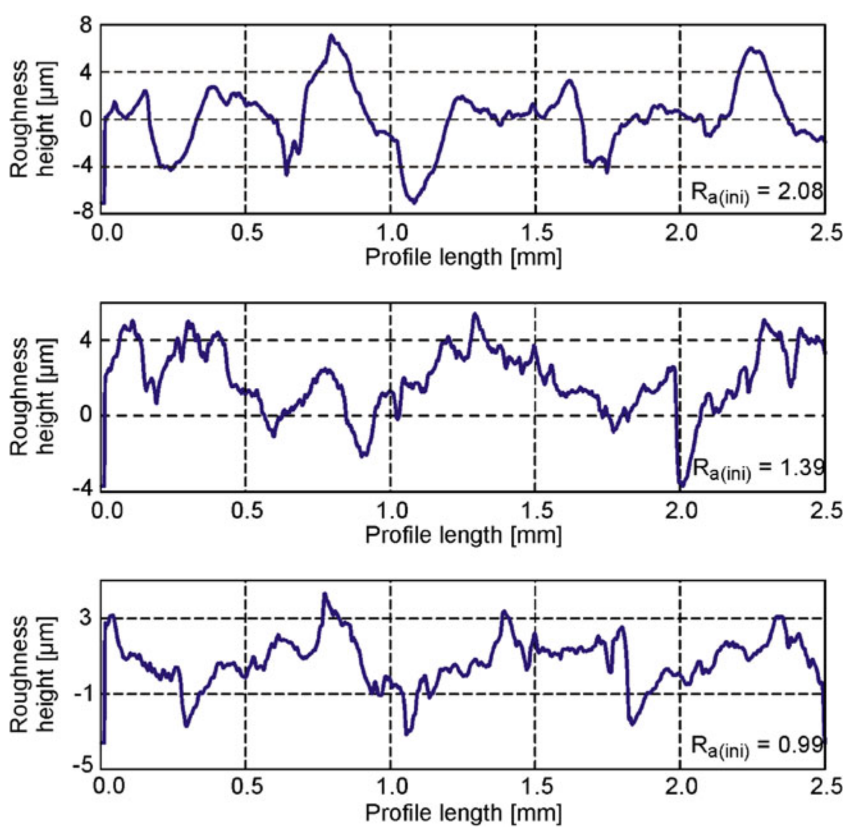

Fig. 4 Surface profiles of the three sections on the plate used in experiment

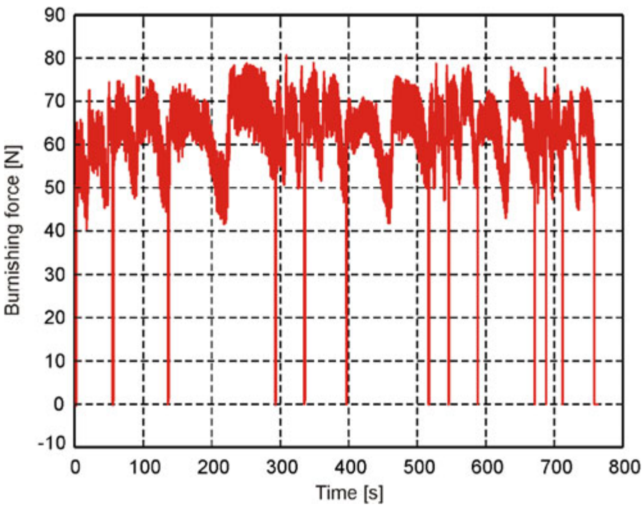

Fig. 5 Example of burnishing force signal recorded for the penetration depth of ≈6 μm

experiment, a 7-mm diameter burnishing ball was made of steel, A 295 52100 (USA/ASTM Ball hardness and surface roughness were 65 HRC, and R_a=0.02 μm, respectively.

The plate was mounted on the clamping plate, type 9443, which was screwed onto the three-component dynamometer, Kistler 9265A, used to measure the forces. The measurements were conducted with three burnishing feeds (f=0.1, 0.2, and 0.3 mm), four numbers of passes, I=1, 2, 3, and 4, and a tool speed of v=2000 mm/min. The forces were varied in the interval of 36.31–383.64 N. Corresponding to these forces were depths of tool penetration along z-axis, in the range of 6–18 μm. Shown in Fig. 5 is a typical example of the force signal, which results in a penetration of approximately 6 μm into workpiece material. Figure 6 shows photo image of the tool performing burnishing operation.

The numerically controlled milling machine was programmed to perform burnishing in 108 fields on the plate with various process regimes, according to the plan of experiment. Nominal force magnitudes were 50, 150, and 300 N. However, due to errors in surface flatness, and initial surface roughness, those values deviated, from field to field, from their nominal values. It is important to note that force deviations did not affect the output results considering that the goal was to perform burnishing with forces, which vary within a defined interval. Presented in Tables 1, 2, and 3 are the results of experimental investigation. For each field, output is the resulting surface roughness R_a (arithmetical mean roughness) and the mean value of bushing force.

To verify the theoretical model, additional experiments were made. These experiments were aimed at identifying the influence of tool system stiffness on the finished surface roughness. Within this segment of experimental investigation,

Fig. 6 Photo image of experiment

Table 1 Measurements of surface roughness parameter, R_a, for initial roughness $R_{a(ini)}$=0.99 μm

I	f_1=0.3 (mm)		f_2=0.2 (mm)		f_3=0.1 (mm)	
	F (N)	R_a (μm)	F (N)	R_a (μm)	F (N)	R_a (μm)
1	53.4	0.264	38.25	0.174	39.72	0.093
2	48.22	0.262	37.84	0.163	42.68	0.17
3	49.68	0.365	41.02	0.167	39.11	0.09
4	44.86	0.207	36.31	0.163	42.41	0.062
1	157.4	0.48	178.9	0.272	187.33	0.07
2	161.81	0.52	182.21	0.269	181.52	0.119
3	176.93	0.5	181	0.33	184.07	0.103
4	177.34	0.537	182.49	0.279	183.2	0.085
1	336.99	0.76	363.14	0.4	383.64	0.125
2	353.84	0.75	371.71	0.397	364.88	0.125
3	368.11	0.79	360.56	0.47	364.67	0.15
4	360.32	0.75	370.31	0.47	370.76	0.12

Table 2 Measurements of surface roughness parameter, R_a, for initial roughness $R_{a(ini)}$=1.36 μm

I	f_1=0.3 (mm)		f_2=0.2 (mm)		f_3=0.1 (mm)	
	F (N)	R_a (μm)	F (N)	R_a (μm)	F (N)	R_a (μm)
1	57.78	0.56	65.6	0.47	63.87	0.16
2	62.5	0.57	63.08	0.34	61.27	0.29
3	65.15	0.38	63.3	0.167	62.84	0.11
4	64.87	0.35	65.67	0.35	62.2	0.09
1	190.41	0.54	202.67	0.317	194.6	0.225
2	199.28	0.575	189.06	0.3	200.95	0.101
3	203.23	0.54	198.68	0.315	204.01	0.111
4	206.87	0.56	198.61	0.38	195.85	0.26
1	300.32	0.71	349.17	0.333	350.35	0.124
2	316.53	0.81	345.13	0.5	363.66	0.17
3	330.38	0.87	353.89	0.46	357.36	0.22
4	349.62	0.86	353.64	0.47	336.74	0.22

Table 3 Measurements of surface roughness parameter, R_a, for initial roughness $R_{a(ini)}$=2.02 μm

I	f_1=0.3 (mm)		f_2=0.2 (mm)		f_3=0.1 (mm)	
	F (N)	R_a (μm)	*F* (N)	R_a (μm)	*F* (N)	R_a (μm)
1	104.86	0.44	96.02	0.23	81.42	0.072
2	101.26	0.431	92.87	0.25	88.27	0.111
3	97.27	0.414	94.7	0.234	86.78	0.085
4	100.8	0.374	92.06	0.221	84.38	0.076
1	173.98	0.56	170.99	0.382	156.15	0.21
2	166.78	0.55	156.25	0.291	179.48	0.067
3	157.34	0.54	182.38	0.29	170.32	0.17
4	182.18	0.51	170.96	0.256	155.11	0.091
1	267.61	0.63	277.64	0.423	256.57	0.072
2	265.8	0.72	252.95	0.301	298.19	0.105
3	251.62	0.68	294.17	0.654	278.03	0.148
4	289.80	0.67	278.44	0.635	253.01	0.138

burnishing force was applied using a system of springs of various stiffnesses. Figures 7 and 8 show the CAD model and photo image of the tool engaged in workpiece material. From Figs. 7 and 8, it is obvious that the burnishing ball, tool carrier, and ball rolling system (consisting of the three radially mounted roller bearings at 120° angle) are identical to those used in the previous experiment. More precisely, the tool system used in the previous experiment was redesigned by implementing a spring and a spring loader. The experiment was performed using springs of k=58.8 N/mm and k=210.5 N/mm stiffness. The quality of previously machined surface was $R_{a(ini)}$=2.02 μm, while the burnishing was performed with feed f=0.2 mm, in a single pass. All other parameters were kept the same as in the previous experiment.

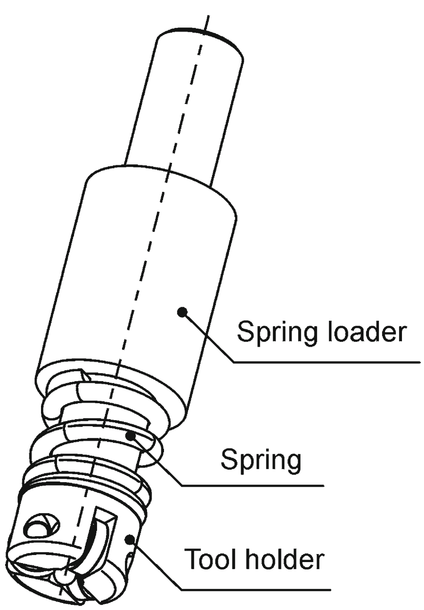

Fig. 7 3D model of the redesigned burnishing tool system

Fig. 8 Photo-image of the redesigned tool system during the process of burnishing

Shown in Fig. 9 is the diagram of dependence of surface roughness, R_a, on the magnitude of burnishing force applied using springs of various stiffness within the tool system. According to the data from Table 3, the diagram also shows the dependence in the case of burnishing with a high-stiffness tool system.

4 Statistical analysis of experimental results

Experimental results obtained by burnishing with high-stiffness tool system were subjected to regression analysis. The data were fitted with power functions. Regression equations and coefficients are shown in Table 4.

Based on regression equations, Fig. 10 shows 3D diagrams of dependence of roughness parameter, R_a, on the burnishing feed and number of passes, for various burnishing forces and initial roughness $R_{a(ini)}$=0.99 μm.

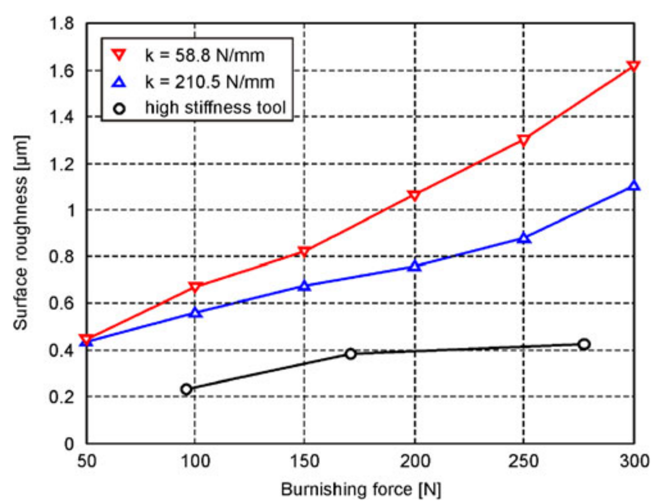

Fig. 9 Dependence of surface roughness, R_a, on the burnishing tool system stiffness, at various burnishing forces

Table 4 Regression equations and coefficients of correlation for experimental data

Initial roughness $R_{a(ini)}$ (μm)	Regression equation	Coefficient of correlation R
2.08	$R_a = 0.024672 \times f^{1.446031} \times I^{0.021286} \times F^{0.920447}$	0.941
1.39	$R_a = 0.616834 \times f^{1.249964} \times I^{0.003332} \times F^{0.290122}$	0.980
0.99	$R_a = 0.63252 \times f^{1.291022} \times I^{0.015914} \times F^{0.277760}$	0.991

Shown in Fig. 11 is a 3D diagram of dependence of roughness parameter, R_a, on the burnishing feed, burnishing force, number of passes and initial roughness.

5 Discussion

Investigations on burnishing process published so far have relied on the tools with springs, which provide constant burnishing force. However, theoretical analysis and experimental results presented in this paper (Fig. 9) show that tool stiffness plays a vital role not only regarding the lower surface roughness but also the dimensional accuracy of the finished part. With this in mind, extensive experimental investigation was conducted with a high-stiffness tool system (Figs. 2 and 6). Based on the diagram in Fig. 9, one can conclude that—all other parameters being the same—higher tool stiffness provides lower surface roughness. Pronounced variations of the burnishing force (Fig. 5) occurred due to tool stiffness. Varying penetration depth of burnishing ball into workpiece material caused variations in burnishing force relative to preset values. For the most part, the disturbances of burnishing force were caused by surface roughness and flatness error, which is also in compliance with the theoretical considerations presented in this paper.

During burnishing experiments, the depth of penetration of high-stiffness tool into workpiece material ranged between 6 and 18 μm. Bearing in mind that these depths are relatively small, the following should be noted:

- Practical implementation of the proposed burnishing method using high stiffness tool system requires a relatively high accuracy of the burnishing ball displacement, i.e., tool positioning. Since modern numerically controlled machine tools provide submicrometer positioning accuracy (up to 0.5 μm) and the depth of burnishing ball penetration is within 6–18 μm range, one concludes that it would be possible to use this penetration depth to control burnishing process with an error that is probably below 10 %.
- Experimental investigations conducted within this study are primarily aimed at clarifying the phenomenon of burnishing with high-stiffness tool. The study showed that burnishing force can be used as one of the key factors in

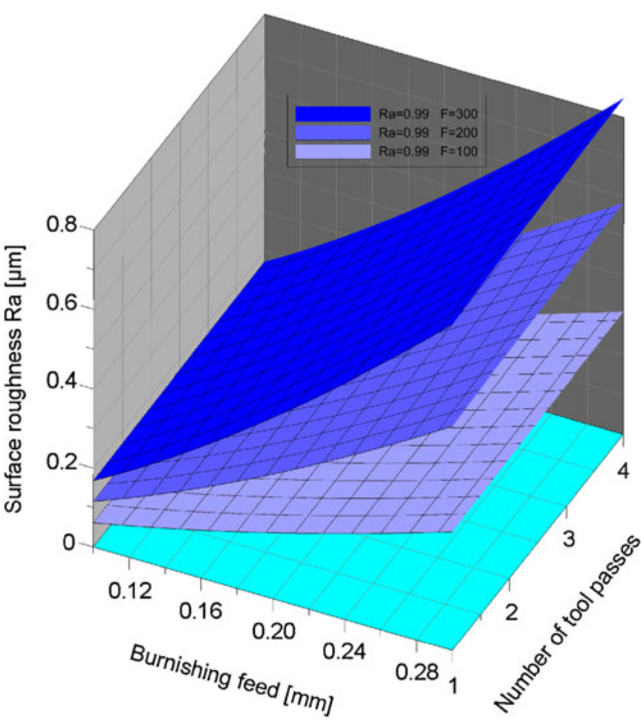

Fig. 10 Trend of R_a change for various burnishing forces, burnishing feeds, and number of passes, at initial roughness $R_{a(ini)}$=0.99 μm

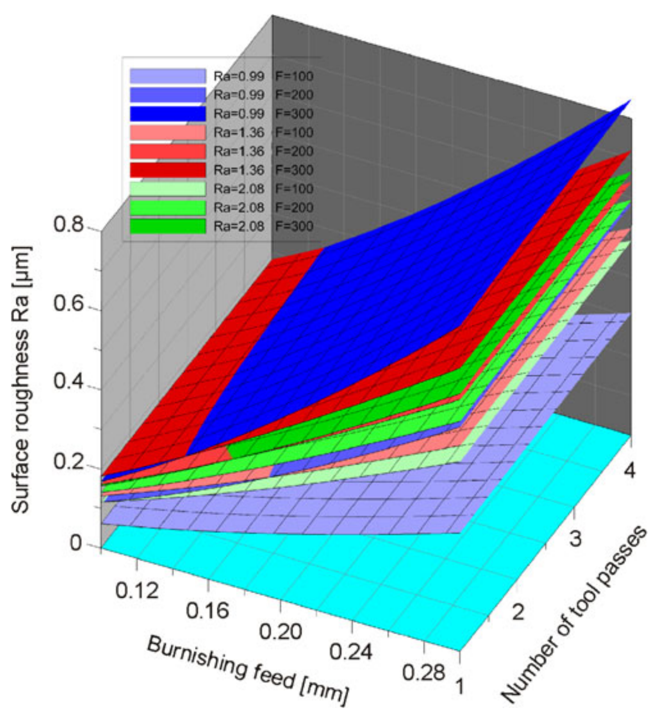

Fig. 11 Trend of R_a change for various burnishing feed, burnishing force, number of passes, and initial roughness

optimization of the burnishing process. Thus, practical industrial application of the proposed burnishing method would require fitting the high-stiffness burnishing tool with a force sensor. This would allow burnishing force to be used as parameter of optimization of the burnishing process, with surface quality as the goal function.

Experimental investigations were conducted as a full experiment, with the burnishing force, burnishing feed, and the number of passes being varied within broad intervals. Burnishing was performed on three machined surfaces of different initial surface roughness. This allowed the forming of regression equations (Table 4) with strong correlation. Based on these power regression equations, one is able to analyze the influence of particular burnishing parameters on the finish surface roughness. For example, judging by the exponents next to the numbers of passes (Table 4), for all three initial surface roughnesses, it is evident that the number of passes exhibits very small influence at any initial surface roughness. The number of burnishing passes is most influential at the initial surface roughness of 2.02 μm. That influence can be assessed if the maximum number of passes (I=4) is raised to the power of 0.021286, which equals 1.02995, and then compared to the unity. Thus, it shows that the influence of the number of burnishing passes on the finish surface quality is <3 %, favoring the larger number of passes. Similarly, regression equations allow one to conclude following:

- Burnishing force of 100 N applied on the surface of initial roughness $R_{a(ini)}$=2.02 μm results in a 63.6 % decrease in finish surface roughness, R_a, compared to that obtained by the burnishing force of 300 N.
- Burnishing force of 100 N applied on the surface of initial roughness $R_{a(ini)}$=1.36 μm results in a 37.54 % decrease in finish surface roughness, R_a, compared to that obtained by the burnishing force of 300 N.
- Burnishing force of 100 N applied on the surface of initial roughness $R_{a(ini)}$=0.99 μm results in a 35.7 % decrease in finish roughness, R_a, compared to that obtained by the burnishing force of 300 N.

The above implies that, on average, smaller burnishing forces yield better reduction of finish surface roughness when applied to surfaces of higher initial roughness.

Based on graphs in Figs. 10 and 11 one concludes that, within entire intervals of burnishing feeds and number of burnishing passes, the smallest surface roughness, R_a, was achieved on the surface of smallest initial roughness, $R_{a(ini)}$=0.99 μm, using a 100 N burnishing force. Moreover, based on the same diagrams, one concludes that the application of burnishing force of 300 N on the surface of smallest initial roughness, $R_{a(ini)}$=0.99 μm, yields larger finish roughness within the entire interval of parameter variation. The largest surface roughnesses, R_a, within the interval of parameter variation, regardless of the initial surface roughness, were produced by the maximum burnishing force of 300 N. Based on the diagrams and regression equations, one concludes that, given the burnishing conditions, lowest R_a's are produced by small burnishing forces (F<100 N) on surfaces of small initial roughness.

The influence of burnishing feed on finish surface roughness is significant. Analysis of regression equations yields following:

- A 0.1-mm burnishing feed on $R_{a(ini)}$=2.02 μm initial roughness decreases finish roughness, R_a, for 79.6 % compared to R_a obtained for a 0.3 mm burnishing feed.
- A 0.1-mm burnishing feed on $R_{a(ini)}$=1.36 μm initial roughness decreases finish roughness, R_a, for 74.67 % compared to R_a obtained for a 0.3 mm burnishing feed.
- A 0.1-mm burnishing feed on $R_{a(ini)}$=0.99 μm initial roughness decreases finish roughness, R_a, for 75.8 % compared to R_a obtained for a 0.3 mm burnishing feed.

This means that, given the experiment conditions, the influence of burnishing feed on finish roughness depends very little on the initial roughness.

Figure 12 presents two identically scaled roughness profiles before and after the burnishing process. Surface roughness prior to the burnishing process equaled $R_{a(ini)}$=0.99 μm. After the burnishing was completed (F=42.41 N, f=0.1 mm, and number of burnishing passes I=3), surface roughness was reduced to R_a=0.062 μm, which is 16 times lower. It is especially important to note that this combination of parameters produced finish quality equivalent to polishing.

It is evident from Fig. 12 that the upper ball surface during burnishing moved very closely to the mean line of the roughness chart. In this way, the roughness peaks

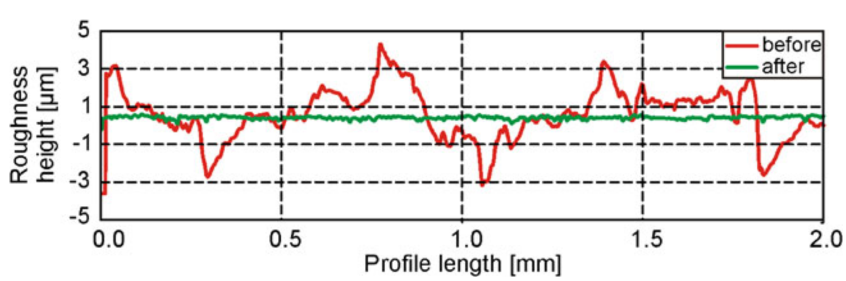

Fig. 12 Surface roughness profiles before and after burnishing

practically filled up the roughness valleys and created a surface of very small roughness, R_a=0.062 μm.

6 Conclusion

Theoretical investigation and experimental results presented in this work showed that tool stiffness significantly affects the finish surface roughness obtained by burnishing. Experimental results confirm the claim that burnishing can be very effectively performed using high-stiffness tool system. This provides advantage to conventional approach regarding the quality of finished surface. In addition, the application of high-stiffness burnishing tools also allows better dimensional accuracy of workpiece, which is a very interesting topic for future research. The results of extensive experimental investigations allowed the forming of regression equations, which provided high correlation between finish roughness, R_a, and most influential burnishing parameters: burnishing force, burnishing feed, number of passes, and initial surface roughness. Based on those regression equations, it was established that burnishing force and burnishing feed significantly affects finish roughness, while the number of burnishing passes does not, which complies with the literature findings. It was also established that initial surface roughness, R_a, and surface profile have significant influence on the effects of burnishing process, especially when the primary goal is to provide high-quality surface finish. For a particular combination of burnishing parameters, a R_a=0.062 μm roughness was produced, which cannot be found in the presently available literature. According to the so far published data, the smallest roughness, R_a=0.19 μm, was obtained for steel AISI 1042, which was previously grinded.

Based on the impact of burnishing force, burnishing feed, and initial roughness, established in this work, the authors maintain that the finish surface quality obtained by burnishing can be significantly increased to match that of polishing. Future investigation shall also be directed towards achieving surface quality whose R_a is close to that of the ball used to perform the burnishing process.

References

1. Gharbi F, Sghaier S, Al-Fadhalah KJ, Benameur T (2011) Effect of ball burnishing process on the surface quality and microstructure properties of AISI 1010 steel plates. J Mater Eng Perform 20:903–910
2. Svalina I, Sabo K, Simunovic G (2011) Machined surface quality prediction models based on moving least squares and moving least absolute deviations methods. Int J Adv Manuf Technol 57:1099–1106
3. Reibenschuh M, Cus F, Zuperl U (2011) Turning of high quality aluminium alloys with minimum costs. Teh Vjesn 18:363–368
4. Lin YC, Wang SW, Lai HY (2004) The relationship between surface roughness and burnishing factor in the burnishing process. Int J Adv Manuf Technol 23:666–671
5. Brinksmeier E, Garbrecht M, Meyer D, Dong J (2008) Surface hardening by strain induced martensitic transformation. Prod Eng 2:109–116
6. El-Taweel TA, El-Axir MH (2009) Analysis and optimization of the ball burnishing process through the Taguchi technique. Int J Adv Manuf Technol 41:301–310
7. Stankovic I, Perinic M, Jurkovic Z, Mandic V, Maricic S (2012) Usage of neural network for the prediction of surface roughness after the roller burnishing. Metalurgija 51:207–210
8. Brinksmeier E, Garbrecht M, Meyer D (2008) Cold surface hardening. CIRP Ann-Manuf Technol 57:541–544
9. Meyer D, Brinksmeier E, Hoffmann F (2011) Surface hardening by cryogenic deep rolling. 1st CIRP Conference on Surface Integrity (CSI), Procedia Engineering, vol 19, pp 258–263
10. Luca L, Neagu-Ventzel S, Marinescu I (2005) Effects of working parameters on surface finish in ball-burnishing of hardened steels. Precis Eng-J Int Soc Precis Eng Nanotechnol 29:253–256
11. El-Axir MH (2000) An Investigation into roller burnishing. Int J Mach Tools Manuf 40:1603–1617
12. Ebeid SJ, El-Taweel TA (2005) Surface improvement through hybridization of electrochemical turning and roller burnishing based on the Taguchi technique. Proc Inst Mech Eng Part B-J Eng Manuf 219:423–430
13. Lin YC, Yan BH, Huang FY (2001) Surface improvement using a combination of electrical discharge machining with ball burnish machining based on the Taguchi method. Int J Adv Manuf Technol 18:673–682
14. Loh HN, Tam CS (1988) Effects of ball burnishing parameters on surfacefinish—a literature survey and discussion. Precis Eng-J Int Soc Precis Eng Nanotechnol 10:215–220
15. Nemat M, Lyons AC (2000) An investigation of the surface topography of ball burnished mild steel and aluminium. Int J Adv Manuf Technol 16:469–473
16. Morimoto T, Tamamura K (1991) Burnishing process using a rotating ball tool—effect of tool material on the burnishing process. Wear 147:185–193
17. Hassan AM, Al-Bsharat AS (1996) Improvement in some properties of non-ferrous metals by the application of the ball burnishing process. J Mater Process Technol 59:250–256
18. Narayan R (1988) Corrosion resistance of ball burnished components. 13th AIMTDR Conference, Jadavpur University, India, pp 6–10
19. Rajaselkariah R, Vaidyanathan S (1975) Increasing the wear resistance of steel components by ball burnishing. Wear 34:183–188
20. Neema LM, Pandy CP (1980) Investigation of the performance characteristic of cold-worked machined surfaces. Wear 60:157–166
21. Hassan AM, Momani AMS (2000) Further improvements in some properties of shot peened components using the burnishing process. Int J Mach Tools Manuf 40:1775–1786
22. Gharbi F, Sghaier S, Hamdi H, Benameur T (2012) Ductility improvement of aluminum 1050A rolled sheet by a newly designed ball burnishing tool device. Int J Adv Manuf Technol 60:87–99
23. Yu XB, Wang LJ (1999) Effect of various parameters on the surface roughness of an aluminium alloy burnished with a spherical surfaced polycrystalline diamond tool. Int J Mach Tools Manuf 39:459–469
24. Luo HY, Liu JY, Wang LJ, Zhong QP (2006) Investigation of the burnishing force during the burnishing process with a cylindrical surfaced tool. Proc Inst Mech Eng Part B-J Eng Manuf 220:893–904
25. Bouzid W, Tsoumarev O, Sai K (2004) An investigation of surface roughness of burnished AISI 1042 steel. Int J Adv Manuf Technol 24:120–125

26. El-Axir MH, El-Khabeery MM (2003) Influence of orthogonal burnishing parameters on surface characteristics for various materials. J Mater Process Technol 132:82–89
27. Salahshoor M, Guo YB (2012) Process mechanics in ball burnishing biomedical magnesium–calcium alloy. Int J Adv Manuf Technol. doi:10.1007/s00170-012-4024-4
28. Prevey SP, Cammett TJ (2004) The influence of surface enhancement by low plasticity burnishing on the corrosion fatigue performance of Al7075-T6. Int J Fatigue 26:975–982
29. El-Axir MH, Othman OM, Abodiena AM (2008) Improvements in out-of-roundness and microhardness of inner surfaces by internal ball burnishing process. J Mater Process Technol 196:120–128
30. El-Khabeery MM, El-Axir MH (2001) Experimental techniques for studying the effects of roller-burnishing parameters on surface integrity. Int J Mach Tools Manuf 41:1705–1719
31. Loh NH, Tam SC, Miyazawa S (1989) A study of the effect of ball-burnishing parameters on surface roughness using factorial design. J Mech Work Technol 18:53–61
32. El-Axir MH, Othman OM, Abodiena AM (2008) Study on the inner surface finishing of aluminum alloy 2014 by ball burnishing process. J Mater Process Technol 202:435–442
33. Hamadache H, Laouar L, Zeghib NE, Chaoui K (2006) Characteristics of Rb40 steel superficial layer under ball and roller burnishing. J Mater Process Technol 180:130–136
34. El-Axir MH, Ibrahim AA (2005) Some surface characteristics due to center rest ball burnishing. J Mater Process Technol 167:47–53
35. Ghafari SH, Golnaraghi F, Ismail F (2008) Effect of localized faults on chaotic vibration of rolling element bearings. Nonlinear Dyn 53:287–301
36. Kapusta H (2004) Analysis of the dynamics of a double-crank driving unit for a needle bench. Fibres Text East Eur 12:83–88